State-of-the-art paper

Bedload transport: a walk between randomness and determinism. Part 1. The state of the art

CHRISTOPHE ANCEY (IAHR Member), Professor*, Civil Engineering Institute/Laboratory of Environmental Hydraulics, École Polytechnique Fédérale de Lausanne, 1015 Lausanne, Switzerland*
Email: christophe.ancey@epfl.ch

ABSTRACT
This paper outlines the various approaches used to calculate bedload transport. As bedload transport exhibits considerable spatial and temporal variations, computing the bedload transport rates and morphological changes experienced by streambeds is difficult. A large body of experimental work has revealed scaling laws relating the mean transport rate q_s to hydraulic conditions (that is, water discharge q_w, bottom shear stress τ_b or stream power ω): $q_s \propto q_w$, $q_s \propto \tau_b^{3/2}$ or $q_s \propto \omega$. The most common approach used to calculate bedload transport has thus long involved determining the one-to-one function $q_s = f(q_w)$ (or any other dependence of q_s on τ_b or ω) from experiments or theoretical considerations. However, the predictive power of such relationships is limited: scientists are unable to predict q_s to within better than one order of magnitude, and morphodynamic models based on $q_s = f(q_w)$ fail to explain the development of bedforms without the use of additional assumptions. Progressively, other calculation approaches have appeared, with many relying on the idea that bedload transport is a macroscopic transport process that primarily reflects random particle motion at the grain scale. The present paper reviews the main ideas being explored today.

Keywords: Bedload transport; bedload transport rate; history of hydraulics; morphodynamics; random motion; stochastic model

1 Introduction

Bedload transport is a specific form of sediment transport, which involves coarse particles (sand, gravel or coarser particles) rolling or saltating along the streambed. In Europe, the increased construction of navigation channels in the eighteenth century gave impetus to the creation of hydraulics – the science of water flow (Levi, 1995). The issue of bed erosion and stability had become progressively more problematic as more channels were built across Europe. The first qualitative description of the erosive action of rivers appeared in 1697 in the book "*Della natura de' fiumi*" (*On the nature of rivers*) by the Italian polymath, Doménico Guglielmini. Today it is largely forgotten, but its influence was significant in the eighteenth century (Simons & Şentük, 1992). At the end of the Little Ice Age, in the nineteenth century, many European countries faced major flooding. For the first time in European history, nationwide mitigation strategies based on river engineering and reforestation were implemented to control water flow on a large scale (Ford, 2016; Vischer, 2003). Rivers and mountain streams mobilizing coarse sediment posed their own specific problems, and these pushed engineers to make the distinction between bedload and suspension. Indeed, bedload transport theory appeared at that time, with the earliest quantitative formulation of a bedload equation usually being attributed to Paul du Boys, a young French engineer studying the Rhone (du Boys, 1879; Hager, 2005, 2009).

This paper outlines the developments in bedload transport theory from du Boys till today. Some recent review papers have covered specific aspects of bedload transport (Hager, 2018; James, Jones, Grace, & Roberts, 2010; Papanicolaou, Elhakeem, Krallis, Prakash, & Edinger, 2008; Wainwright et al., 2015), but the topic is vast, and I will mainly give a hydraulic perspective. In a companion paper (Ancey, 2020), I outline some of the key challenges and prospects for bedload transport calculation. Additional material is provided in the online supplemental material (see the public data repository figshare: https://doi.org/10.6084/m9.figshare.9892118), including three videos showing bedload transport experiments.

2 A brief historical overview

2.1 *Empirical bedload transport equations*

The starting point for bedload transport theory was the speculative analysis conducted by du Boys (1879). He envisioned bedload transport as continuous layers of grains sliding against each other under the tractive force of water. Assessing the forces experienced by these layers led him to propose the prototypical bedload transport equation:

$$q_s = \chi \tau_b (\tau_b - \tau_c) \tag{1}$$

where q_s is the bedload transport rate per unit width, τ_b denotes the bottom shear stress, τ_c is the critical shear stress above which layers start sliding, and χ is a material coefficient. Du Boys introduced two elements that have been commonly used in bedload transport equations since then: (i) the bedload transport rate depends on bottom shear stress; and (ii) bed layers only start to move when the bottom shear stress exceeds a critical value (du Boys, 1879).

Another vision of bedload transport developed in the twentieth century with the work of Armin Schoklitsch and Ralph Bagnold: bedload transport was considered to be driven by excess power rather than excess shear stress. Schoklitsch formulated his bedload equation using the waterway's water discharge:

$$q_s = 1.5i^{3/2}(q_w - q_c) \tag{2}$$

where q_w denotes the water discharge per unit width, i is the bed slope, and q_c is a critical discharge. Equation (2) can also be interpreted in terms of stream power ω (per unit width) as $\omega = \tau_b \bar{u} = \rho g q_w i$ under steady-state, uniform-flow conditions, where $\bar{u}$ denotes the depth-averaged water velocity, ρ is water density, and g is gravitational acceleration. Taking advantage of his experience with granular flows and aeolian transport, Bagnold (1956) provided new physical insights into bedload transport. Bagnold argued that a water stream behaves like an energy reservoir: most of the energy supplied by the gravitational acceleration is dissipated by turbulence, but when the bottom shear stress τ_b exceeds the critical shear stress τ_c, the excess of energy $(\tau_b - \tau_c)\bar{u}$ is available to bedload particles and is imparted to them via momentum exchanges. He ended up with the relation:

$$q_s = \frac{a u_*}{\cos \theta}(\tau_b - \tau_c) \tag{3}$$

where a is a material coefficient (depending on particle density and angle of repose), θ is bed inclination, and $u_* = \sqrt{\tau_b/\rho}$ is called the friction velocity. In his quest for a universal law of sediment transport, Bagnold gradually abandoned the "principles of physics" claimed in his earlier papers and eventually used empirical arguments to simplify Eq. (3):

$$q_s = e_b \bar{u} \tau_b \tan \alpha = e_b \omega \tan \alpha \tag{4}$$

where e_b is the bedload transport efficiency factor and α is the dynamic friction coefficient (Bagnold, 1980, 1986). Bagnold made little comment about his change of paradigm. One presumes that he became increasingly aware of the shortcomings in his theoretical model – as identified later by several authors (Bailard & Inman, 1979; Seminara, Solari, & Parker, 2002) – and progressively leaned toward a purely empirical approach. Although Bagnold's empirical approach is reasonably successful at calculating transport rates for a wide range of flow conditions (Bagnold, 1980, 1986; Lammers & Bledsoe, 2018; Martin, 2000), there are legitimate questions about its accuracy. The impressively good fit displayed in his papers was obtained by discarding certain data without any clear motivation (Martin, 2000), and similar fits were not observed for other datasets.

Bagnold's attempt to find a correlation between bedload transport rate and water discharge/stream power eventually led him to use the common approach, taken since the early twentieth century, which involved fitting regression equations to field or laboratory data. Many of them are still routinely used, such as the Meyer-Peter–Müller equation (MPM), which, in the absence of correction factors, is expressed as (Meyer-Peter & Müller, 1948; Wong & Parker, 2006):

$$\Phi = 8(\Theta - \Theta_c^*)^{3/2} \text{ with } \Phi = \frac{q_s}{d\sqrt{gRd}} \text{ and } \Theta = \frac{\tau_b}{\rho Rgd} \tag{5}$$

where $R = \rho_s/\rho - 1$ is the density ratio, ρ_s is sediment density, $\Theta_c^* = 0.047$ is the dimensional critical shear stress, and d is the mean particle diameter. Equation (5) also defines the dimensionless bedload transport rate Φ and the Shields number Θ. Several equations have been built using the same principle (e.g. Recking, 2013; Rickenmann, 1990; Smart & Jaeggi, 1983).

2.2 *Einstein's statistical approach*

A turning point in the development of bedload theory was the work done by a young PhD student: Hans Albert Einstein was initially hired to work on bedload transport in the Alpine Rhine under the supervision of Meyer-Peter at the ETHZ/VAW (the Laboratory of Hydraulics, Hydrology and Glaciology at ETH Zurich). Faced with the failure of existing empirical equations, Meyer-Peter thought that it would be worth refining them by including more dependent variables, such as particle diameter (Meyer-Peter, Favre, & Einstein, 1934), but Einstein saw things differently. Observing random particle paths in a flume, Einstein concluded that randomness was a key feature of bedload transport (Ettema & Mutel, 2014), and he then undertook to study "bedload transport as a probability problem" (Einstein, 1937). Einstein initially drew an analogy between the random path of

a particle across a Galton board and the intermittent motion of bedload in a flume.

In the years following his move to the USA, Einstein revisited the initial problem. He assumed that turbulence gave rise to fluctuations in the lift force, and that over a certain period t_e there was a probability p that the lift force exceeded the particle weight, causing the particle to move. Let us consider a control volume whose length matches the mean distance $\bar{l}$ travelled by a particle between two states of rest. The volume contains n spherical particles (of diameter d), and the number of particles dislodged over time t_e is thus pn. The entrainment rate is thus $E = \alpha_v pnd/t_e$ (where $\alpha_v d$ represents the particle volume per unit bed area). Einstein assumed that the deposition rate in this control volume was proportional to the particle transport rate q_s: $D = q_s/\bar{l}$. Under steady-state conditions, the deposition rate D matches the erosion rate E, and thus the particle transport rate is:

$$q_s = \frac{\alpha_v pnd\bar{l}}{t_e} \qquad (6)$$

To close this equation, Einstein assumed that time t_e (called the exchange time) was related to the particle settling velocity v_s:

$$t_e \propto \frac{d}{v_s} = k\sqrt{\frac{\rho d}{g(\rho_s - \rho)}} \qquad (7)$$

where k is a (dimensionless) constant. The mean travelled distance $\bar{l}$ is related to the entrainment probability p and leap length l. Let us assume that at a given time, n particles are entrained along the stream. On average, after leaping over length l, $(1-p)n$ particles are deposited whereas pn continue to move. Among these moving particles, $p(1-p)n$ are deposited after travelling distance $2l$, whereas $p^2 n$ are still moving, and so on. The mean distance travelled is then $\bar{l} = \sum_{n=0}^{\infty}(1-p)p^n l = l(1-p)^{-1}$. Using these considerations, he derived the transport rate equation:

$$q_s = \frac{nld\alpha_v}{k}\sqrt{\frac{g(\rho_s - \rho)}{\rho d}}\frac{p}{1-p} \qquad (8)$$

or put into a dimensionless form:

$$\Phi = q_s\sqrt{\frac{\rho}{(\rho_s - \rho)}\frac{1}{gd^3}} = \alpha\frac{p}{1-p} \qquad (9)$$

where α groups the constants together: $\alpha = nl\alpha_v/(kd)$. The probability of entrainment p depends on the buoyancy-to-lift-force ratio:

$$p = f\left(\frac{(\rho_s - \rho)gd^3}{c_l\rho d^2 u_*^2}\right) \qquad (10)$$

where c_l denotes the lift coefficient, u_* is the friction velocity, and f is a function to be determined. Einstein (1942) defined the flow intensity $\Psi = (\rho_s - \rho)gd/(\rho u_*^2)$ (which is the inverse

of the Shields number Θ), and derived the dimensionless form of Eq. (10): $p = f(\Psi)$. He thus obtained an implicit relation for the bedload transport rate:

$$p = \frac{1+\Phi}{\alpha+\Phi} = 1 - \frac{1}{\sqrt{\pi}}\int_{-a_1\Psi - a_2}^{a_1\Psi - a_2}e^{-\xi^2}\,d\xi \qquad (11)$$

By solving this implicit equation numerically, Einstein was able to deduce the bedload transport rate from the probability of entrainment p. The constants α, a_1 and a_2 were obtained by fitting the $\Phi(\Psi)$ curve to the data obtained by Meyer-Peter and Gilbert Murphy (1914): $a_1 = 0.156$, $a_2 = 2.0$, and $\alpha = 1/27$. Einstein's equation led to two noticeable achievements. First, Einstein's bedload equation $\Phi(\Psi)$ is in remarkable agreement with the Meyer-Peter–Müller Eq. (5), as shown in Fig. 1. Admittedly, Einstein used Meyer-Peter's data to fit his Eq. (11), but his equation is a general expression with only three parameters, and the good match covers five orders of magnitude of Φ. Second, he showed that using the right dimensionless groups made it possible to collapse all the experimental data onto a single curve which is closely described by Eq. (11).

The recent literature has often credited Hans Albert Einstein as being the father of random-walk and stochastic models of bedload. Indeed, we can consider that his doctoral work (Einstein, 1937) pioneered random-walk models even though the formalism used differed from the modern theory of random walks (e.g. Schumer, Meerschaert, & Bauemer, 2009). His later work on bedload transport cannot be viewed as a stochastic (or even probabilistic) approach: although he used statistical arguments, these remained heuristic considerations, and he did not calculate any probability distributions of bedload transport rates (or of any other quantity). Einstein nevertheless sowed seeds that were reaped many years later: his seminal papers have been revisited by a number of authors (Ancey, Böhm,
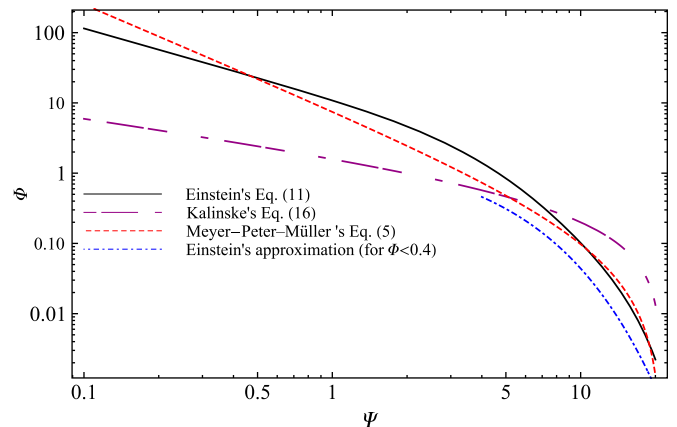

Figure 1 Comparison of Einstein's bedload equation $\Phi(\Psi)$ with the Meyer-Peter–Müller Eq. (5). For Einstein's equation, we use the definition of Φ given by Eq. (9) and the dependence of p on Ψ given by Eq. (11). Meyer-Peter's Eq. (5) can be expressed in terms of Ψ and Φ: $\Phi = (4/\Psi - 0.188)^{3/2}$ (Graf, 1984). The blue dot-and-dash curve shows the empirical equation $0.456\Phi = e^{-0.391\Psi}$ obtained by Einstein (1942) and valid for $\Phi < 0.4$

Jodeau, & Frey, 2006; Armanini, 2018; Armanini, Cavedon, & Righetti, 2014; Lisle et al., 1998; Yalin, 1972) and have given rise to numerous concepts still in widespread use today (e.g. bedload transport as an intermittent process, dimensional analysis, probabilities of entrainment and deposition, influence of turbulence on incipient motion).

2.3   *Kalinske's mechanical approach*

At nearly the same time as Hans Albert Einstein, Anton Kalinske developed a simple theory of bedload transport which put the emphasis on particle motion (Kalinske, 1947). Kalinske (1947) defined the bedload transport rate from the volume of particles in motion (per unit streambed area) γ and their mean velocity $\bar{u}_p$:

$$q_s = \gamma \bar{u}_p \tag{12}$$

where γ is today called the particle activity, and the mean particle velocity is:

$$\bar{u}_p = \int_{u_c}^{\infty} b(u - u_c)f(u)\,\mathrm{d}u \tag{13}$$

where u denotes the fluid velocity at the grain level, u_c is the critical fluid velocity (related to incipient motion), $f(u)$ is the probability density function of fluid velocity, and b is a constant which should be close to unity. In other words, Kalinske assumed that particle velocity adapted instantaneously to fluid velocity. He further assumed that (i) $f(u)$ was the normal distribution with mean $\bar{u}$ and variance σ^2; (ii) the critical velocity was proportional to the time-averaged fluid velocity at the grain level $\bar{u}_b$: $u_c = \bar{u}\sqrt{\tau_c/\tau_b}$ where τ_c was the critical (Shields) shear stress and τ_b was the bed shear stress; and (iii) $\bar{u}_b$ was proportional to the friction velocity $u_* = \sqrt{\tau_b/\rho}$: $\bar{u}_b = cu_*$ with $c \sim 11$. With these assumptions, the bedload transport rate of Eq. (12) becomes:

$$q_s = \gamma b\bar{u} \int_{\xi_c}^{\infty} (\xi - \xi_c)\tilde{f}(\xi)\,\mathrm{d}\xi \tag{14}$$

where $\xi_c = \tau_c/\tau_b$ and $\tilde{f}$ is the normal distribution of mean unity and scaled standard deviation $r = \sigma/\bar{u}$. When the bottom shear stress is sufficiently large relative to the critical Shields stress (that is, for $\xi_c \to 0$), a first-order power expansion in ξ_c and r shows no dependence of q_s on r:

$$q_s = \gamma b\bar{u}(1 - \xi_c) \tag{15}$$

or in a dimensionless form:

$$\Phi = \frac{\gamma bc}{d}\left(\frac{1}{\sqrt{\Psi}} - \frac{1}{\sqrt{\Psi_c}}\right) = \frac{\gamma bc}{d}(\sqrt{\Theta} - \sqrt{\Theta_c}) \tag{16}$$

The bedload transport rate q_s is closely approximated by the linear trend Eq. (15) for $\xi_c \leq 0.4$. Under laminar flow conditions

($r = 0$), the bedload transport rate q_s matches the linear function Eq. (15), and for $\xi_c > 1$ (that is, for $\tau_b < \tau_c$) there is no bedload transport. For turbulent flows, however, weak sediment transport occurs for $\xi_c > 1$. In his only paper devoted to bedload transport, Kalinske (1947) considered particle activity to be constant (with $\gamma = 0.35$ moving particles per unit streambed area). In his model, bedload transport was entirely driven by particle velocity Eq. (13), which was controlled by water velocity. Although Kalinske (1947) obtained a good agreement between Eq. (14) and Meyer-Peter's data, a comparison between the MPM Eq. (5) and Kalinske's Eq. (16) shows that they roughly overlap each other for $\Psi > 5$ (Fig. 1). For intense sediment transport ($\Psi \to 0$), Kalinske's Eq. (16) scales as $\Psi^{-1/2}$ whereas Meyer-Peter's Eq. (5) varies as $\Psi^{-3/2}$. The assumption of constant particle activity probably explains this difference between the two models.

Kalinske's approach predicts a linear dependence of mean particle velocity on water velocity, in agreement with experimental measurements for saltating particles (Ali & Dey, 2019), but when particles are rolling and saltating, the relationship between particle and water velocities is more complicated (Ancey, Bigillon, Frey, & Ducret, 2003). The weak influence of particle inertia on particle velocity has also been verified for saltating particles (Heyman, Bohorquez, & Ancey, 2016).

The main shortcoming in Kalinske's (1947) approach was ignoring the variations in particle activity. Decades later, Wiberg and Smith (1989) developed an approach similar to Kalinske's, but taking this missing element into account. They showed that γ should vary with the stress difference $\tau_b - \tau_c$. This then leads to a scaling of Eq. (16) that matches the MPM Eq. (5). Combining theoretical elements from Einstein's theory and experimental data, Fernandez Luque and van Beek (1976) also found that particle activity should scale as $\tau_b - \tau_c$, and they concluded that Kalinske's assumption was an oversimplification. Despite its shortcomings, Kalinske's work attracted growing attention from the 1970s onward. Experimentally, it became possible to track individual particles and measure their velocities (Ali & Dey, 2019). Theoretically, the idea of calculating the fate of individual particles experiencing hydrodynamic forces and jumps became appealing. Charru, Mouilleron, and Eiff (2004) and other authors developed models following Kalinske's seminal ideas (Section 4.2).

2.4   *The part played by bedforms*

In the 1930s, field measurements revealed temporal variability in sediment transport rate records, with a sometimes remarkable periodicity in peak values which was interpreted as dune migration (Gomez, 1991). In the 1960s, scientists took a closer look at bedload transport rates induced by dune migration. Simons, Richardson, and Nordin (1965) considered bedforms (ripples, dunes) migrating downstream at a constant velocity c and featuring a triangular longitudinal profile of height δ. Using the Exner

equation:

$$(1 - \zeta)\frac{\partial y_b}{\partial t} = -\frac{\partial q_s}{\partial x} \qquad (17)$$

where ζ denotes bed porosity and y_b is bed elevation, then making the change of frame $\xi = x - ct$ to track dune motion, they turned the Exner Eq. (17) into an ordinary differential equation:

$$(1 - \zeta)c\frac{\mathrm{d}y_b}{\mathrm{d}\xi} = \frac{\mathrm{d}q_s}{\mathrm{d}\xi} \qquad (18)$$

whose integration gives: $q_s = (1 - \zeta)cy_b + a$, where a is a constant of integration set to zero thereafter. Integrating this rate over the dune length, they obtained the space-averaged transport rate (Richardson, Simons, & Posakony, 1961; Simons et al., 1965):

$$\bar{q}_s = \frac{1}{2}(1 - \zeta)V\delta \qquad (19)$$

Hamamori (1962) was more interested in the transport rate fluctuations induced by bedform migration. Assuming a superposition of triangular-shaped structures (from ripples to dunes), he deduced that the bedload transport rate fluctuations could be described by the finite-support probability distribution $f(q_s)$:

$$f(q_s) = \frac{4}{\bar{q}_s}\ln\left(\frac{4\bar{q}_s}{q_s}\right) \qquad (20)$$

for $0 < q_s \le 4\bar{q}_s$, where $\bar{q}_s$ is the mean transport rate. By definition, the mean value is $\bar{q}_s$, whereas the variance is $7\bar{q}_s^2/9$.

The framework developed by Simons et al. (1965) and Hamamori (1962) seems to offer a simple way of calculating the bedload transport rate and its fluctuations. The difficulty lies in identifying the height scale δ and migration celerity V. Careful examinations of sand dunes have converged to show that bedforms do not show any regularity in terms of size, shape or spacing, even for well-sorted sediment under steady-state conditions in one-directional flows (Hino, 1968; Nikora, Sukhodolov, & Rowinski, 1997; Nordin & Algert, 1966; van der Mark, Blom, & Hulscher, 2008). Bedforms are not travelling waves moving at a constant unique speed V: rather they evolve continuously, changing shape and velocity over time, and with scale dependence of their migration speed (Guala, Singh, BadHeartBull, & Foufoula-Georgiou, 2014; Nikora et al., 1997; Singh, Lanzoni, Wilcock, & Foufoula-Georgiou, 2011). The Hamamori distribution Eq. (20) predicted fluctuations whose maximum amplitude was $4\bar{q}_s$. In laboratory experiments, fluctuations as large as $10\bar{q}_s$ have been observed, and this could not be explained entirely by bar migration (Dhont & Ancey, 2018).

3 The state of the art: macroscopic behaviour

3.1 *The minimal system*

To develop the simplest physical view of bedload transport, we consider a one-dimensional steady-state flow over a granular bed of indefinite length, tilted at angle θ to the horizontal. Far upstream, the water discharge q_w is constant. Sediment is transported at an average constant rate $\bar{q}_s$ (as will be illustrated by Fig. 1 in the companion article (Ancey, 2020), the exact meaning of "average" in terms of timescale is more complicated than it first appears, but this will not be examined here). The sediment is composed of particles of similar size. The hyporheic flow through the granular bed is neglected. The bed is initially flat, and the flow depth h is uniformly constant.

The first step is to define what bedload transport means. It is usual to distinguish between *suspended sediment* and *bedload*. Suspended particles are those maintained in suspension in the stream by turbulence, with no contact with the bed. By contrast, bedload involves particles moving along the bed, with continual (by rolling) or intermittent (by saltating) contact. This distinction may seem simple on paper, but observing it closely in experiments or integrating it into image processing algorithms raises difficulties. Issues such as differentiating between jiggled resting and rolling states lead to marginal errors, but other issues are more difficult to determine. At low sediment transport rates, many particles move individually, but some move collectively, forming coherent ensembles of particles. It is tempting to call these ensembles *sediment waves*, but as this expression has been used in various other contexts, it may be ambiguous (Lisle, 2004). As shown in the accompanying video (in the online supplemental material), these sediment waves may move more slowly than isolated particles, and thus they may be viewed as the bed's slow, creeping motion driven by sediment transport. They may also move as granular flows (*en masse*), with a thickness spanning several particle diameters and a velocity that matches that of isolated particles. These flows frequently occur in the form of avalanches from the bed's banks or a dune's lee side, but they are also observed when bedforms suddenly release fixed volumes of sediment (Dhont & Ancey, 2018). At high sediment transport rates, many particles move collectively; they form a shallow layer of rolling and saltating particles, which is closer to a granular gas than a coherent dense granular carpet. Differentiating the various forms of motion has proven to be difficult because of the overlapping time and length scales they display.

The second step is to define the bedload transport rate Q_s. A number of expressions have been proposed, serving different purposes depending on the experimental constraints (Ballio, Nikora, & Coleman, 2014; Ballio, Pokrajac, Radice, & Hosseini Sadabadi, 2018; Campagnol, Radice, & Ballio, 2012; Furbish, Haff, Roseberry, & Schmeeckle, 2012). In fluid mechanics, it seems natural to define the flux of particles Q_s across a control surface S:

$$Q_s(t) = \int_S H(\boldsymbol{x})\boldsymbol{u_p} \cdot \boldsymbol{n}\,\mathrm{d}S \qquad (21)$$

where $\boldsymbol{n}$ denotes the unit normal to the control surface and H is the phase-indicating function: $H(\boldsymbol{x}) = 1$ when $\boldsymbol{x}$ lies inside a particle, and $H(\boldsymbol{x}) = 0$ when $\boldsymbol{x}$ lies in the carrying fluid. This

definition turns out to be difficult to apply either experimentally or theoretically. In practice, it is possible to count the number of particles crossing a surface by using, for instance, image processing or geophones, but this is done by counting the number of particles that have crossed the surface over a period of time δt, not by measuring the instantaneous flux. Various definitions based on time- or space-averaging have been substituted for Eq. (21) (online supplemental material).

Simons et al. (1965) provided another perspective, emphasizing the part played by bedforms in bedload transport rates. Equation (19) has been extended to reflect the multiscale nature of bedform (Guala et al., 2014; Nikora, 1984):

$$q_s = (1 - \zeta) \int_{k_{\min}}^{k_{\max}} A(k)C(k)\, \mathrm{d}k \qquad (22)$$

According to Eq. (22), a bedform profile is interpreted as a linear superposition of sinusoids of wave number $k = 2\pi/\lambda$, whose propagation speed $C(k)$ is scale dependent. Thus, each sinusoid's contribution to the total bedload is defined as a product of its amplitude $A(k)\, \mathrm{d}k$ and speed of propagation $C(k)$, where $A(k)$ is an amplitude spectral density of the bed profile.

In addition to the approaches viewing bedload transport as a continuum, there are approaches that focus on the "fate" of individual particles. To monitor how particles spread along a flume, Einstein (1937) painted particles different colours, and using these tracers subsequently became quite common, especially in field surveys (Section 5.3). Under bed-equilibrium conditions, Einstein (1950) defined the sediment transport rate as:

$$q_s = E\bar{l} \qquad (23)$$

where $\bar{l}$ is the mean length travelled by individual particles during each leap (Section 2.2). Several field measurement campaigns used Einstein-like definitions to monitor bedload transport under incipient-motion conditions (Wilcock, 1997); laboratory experiments and theoretical analyses made extensive use of this definition (Fernandez Luque & van Beek, 1976; Seminara et al., 2002). From the observation that particles can be moving, lying at rest on the bed surface or buried in the bed, we can define a virtual velocity U_p (that is, the displacement-to-time ratio, when the time considered is sufficiently long to involve both resting and motion phases) for an individual particle. Only the upper bed layer participates in bedload transport, and it is therefore termed the active layer (e.g. Church & Haschenburger, 2017); the thickness of this layer is denoted by L_a and represents the depth down to which the bed is continuously reworked by fill and scour. Mass conservation then implies that:

$$q_s = U_p L_a \qquad (24)$$

This equation has been used for both natural rivers (Ferguson, Bloomer, Hoey, & Werritty, 2002) and flume experiments (Ganti, Meerschaert, Foufoula-Georgiou, Viparelli,

& Parker, 2010; Wong, Parker, DeVries, Brown, & Burges, 2007).

3.2   *Interplay and feedback loops*

The physical representation drawn in the preceding subsection is helpful to define bedload transport, but it may be misleading because it regards sediment transport as an isolated system whose variations are dictated solely by the water flow, rather than the dynamic interplay between the stream, the bed and the bedload.

The stream carries grains dislodged from the bed by imparting part of its momentum to them. An initially planar streambed quickly develops grain patches, which ultimately form larger structures called bedforms. In turn, these bedforms affect how turbulence is generated within the flow and how energy is dissipated. This leads to complex interplay between the grains, the bed surface and the water flow. Initial disturbances to the stream surface are amplified by sediment transport and turbulence, but this growth is not indefinite. There are thus positive and negative feedback loops at work in the development of bedforms. There is such a tremendous wealth of forms (Blondeaux, Colombini, Seminara, & Vittori, 2018) that it is impossible to explain their origins by a single mechanism.

Bedforms such as dunes and anti-dunes have often been considered the signatures of streambed instability. Linear stability analysis is the standard tool for studying the conditions necessary for the development of instabilities. The simplest set of equations enabling the implementation of this tool is a combination of the shallow water (or Saint-Venant) equations for the mass and momentum balance equation of the water stream:

$$\frac{\partial h}{\partial t} + \frac{\partial h\bar{u}}{\partial x} = 0 \qquad (25)$$

$$\frac{\partial h\bar{u}}{\partial t} + \frac{\partial h\bar{u}^2}{\partial x} + gh\frac{\partial h}{\partial x} = -gh\frac{\partial y_b}{\partial x} - \frac{\tau_b}{\rho} + \frac{\partial}{\partial x}\left(\nu h \frac{\partial \bar{u}}{\partial x}\right) \quad (26)$$

and the Exner equation for the mass balance of the bed (when the suspended load is neglected):

$$(1 - \zeta)\frac{\partial y_b}{\partial t} = D - E = -\frac{\partial q_s}{\partial x} \qquad (27)$$

in which $h(x,t)$ denotes the flow depth, $y_b(x,t)$ is the bed elevation, $\bar{u}$ is the depth-averaged velocity, x is the downstream position, t is time, ρ is the water density, τ_b is the bottom shear stress, ζ is the bed porosity, D and E represent the deposition and entrainment rates, respectively, and ν is the eddy viscosity. The bed slope is defined as $\tan\theta = -\partial_x y_b$. The governing equations are closed by empirical relationships for the flow resistance τ_b and bedload transport rate q_s, which are assumed to depend on the flow variables $\bar{u}$ and h and other additional parameters (e.g. bed roughness and slope).

The linear stability analysis involves starting from a steady-state uniform flow ($h(x,t) = H$, $u(x,t) = U$, and $y_b(x,t) =$

0) over a flat bed and then perturbing this "base" solution $(h, u, y_b) = (H, U, 0) + (h', u', y_b')$. After linearizing Eqs (25)–(27) and expressing the disturbances as normal modes, that is, with an exponential dependence on space and time $(h', u', y_b') \propto \exp[ik(x - ct)]$ (where k is the wavenumber and c is bed wave speed), we obtain the dispersion relation, which here is a third-order polynomial for $c(k)$. The imaginary part c_i of the solution $c = c_r + ic_i$ to this equation determines the stability of the disturbances, and they are only stable if $c_i < 0$. The first two solutions to the dispersion equation are called the hydrodynamic modes as they describe the propagation of fast-evolving water waves. They are barely modified by the erodible bed (Balmforth & Provenzale, 2001; Bohorquez, Cañada Pereira, Jimenez-Ruiz, & del Moral-Erencia, 2019), and they are thus stable for Froude numbers F lower than 2. The third solution to the dispersion equation is called the sediment mode because it describes the bed's slow evolution. This mode is stable when empirical bedload equations q_s are explicit one-to-one functions of $\bar{u}$ and h (Balmforth & Provenzale, 2001; Bohorquez et al., 2019). The only effect of bedload transport is to slightly alter the dynamics of water waves.

Various reasons have been proposed to explain why the Saint-Venant–Exner equations fail to generate bedforms when F < 2:

- The first and probably the most commonly proposed explanation is that the Saint-Venant Eqs (25)–(26) are too simple to account for the interplay between the turbulent flow and bed surface. Classic flow resistance equations, in the form of $\tau_b(\bar{u}, h)$, are often blamed for the failure to provide the instability criterion because they lead to bottom drag in phase with the velocity (Charru, 2006; Colombini, 2004; Fourrière, Claudin, & Andreotti, 2010) when a phase lag is expected, as shown, for instance, by the analytical study of Newtonian fluids over a wavy bed. One strategy to remedy this failure is to introduce a spatial or temporal lag into the relationship $q_s(\bar{u}, h)$. For instance, Colombini (2004) defined the bed shear stress at the interface between the saltation layer and the flow (instead of the bed surface).
- Another possible explanation is that bedforms arise from the coalescence of ripples in a two-stage process (Coleman & Melville, 1994). In stage one, turbulent eddies (mainly sweep-transport events) cause groups of particles to be collectively entrained and convected by the flow. In stage two, interacting grain patches form bed disturbances, which may locally disrupt bedload transport, causing particles to pile up and the disturbance to grow (Coleman & Nikora, 2011).
- The third possible explanation is that one-to-one bedload transport equations $q_s = q_s(h, \bar{u})$ do not incorporate the necessary physics. As the next section shows, recent models have expressed bedload transport as the solution to an ordinary differential equation (Sections 4.1 and 4.2) or have added a diffusive term to it (Sections 4.3 and 4.4), breaking the one-to-one relationship with the flow variables. In both cases,

the change to the definition of q_s has led to more realistic predictions of unstable modes.

4 Mass-balance models

The Exner Eq. (27) has been central to many developments in hydraulics and the morphodynamics of rivers. It has been derived using different approaches and used in different contexts, including soil erosion and landscape dynamics (Coleman & Nikora, 2009; Exner, 1925; Paola & Voller, 2005). It expresses the bed's mass conservation from two perspectives (Furbish, Fathel, & Schmeeckle, 2017; Parker, Paola, & Leclair, 2000):

- In the so-called entrainment form, differences between the entrainment and deposition rates (E and D) lead to time variations in the bed elevation y_b. Although the Exner Eq. (27) involves the two processes of entrainment and deposition (through their rates E and D), these processes are not independent. Indeed, Tsujimoto showed that:

$$D(x, t) = \int_{-\infty}^{t} \int_{-\infty}^{x} E(x - r, t - \tau) f(x, t | x - r, t - \tau) \, dr \, d\tau$$

(28)

where f denotes the probability density that a particle, once entrained from $x - r$ at time $t - \tau$, travels a distance r before being deposited at x (Nakagawa & Tsujimoto, 1980). Similarly, the bedload transport rate can be defined as the flux of particles entrained from $x - r$:

$$q_s(x, t) = \int_{-\infty}^{t} \int_{-\infty}^{x} E(x - r, t - \tau) F(r; t | x - r, t - \tau) \, dr \, d\tau$$

(29)

where F is the exceedance probability that the particle jumps by at least r between times $t - \tau$ and t (Nakagawa & Tsujimoto, 1980).

- In the flux form, the spatial gradient in the bedload transport rate gives rise to time variations in the bed elevation. It can be shown that the two forms are strictly equivalent: differentiating Eq. (29) with respect to x leads to $\partial_x q_s = E - D$ (Parker et al., 2000).

The Exner equation has been the starting point for several models developed to compute bedload transport rates, as we shall examine in detail below.

4.1 *The Parker–Paola–Leclair model (2000)*

A revival of interest in stochastic and probabilistic models occurred in the 2000s, notably with the probabilistic formulation of the Exner equation proposed by Parker et al. (2000). The authors' essential motivation was to find a substitute to the concept of active layer. They assumed that under steady-state conditions, the bedforms could be fully described by the bed

elevation's probability density function $f(y)$. The probability that the bed elevation falls within the elevation range $[y, y + \mathrm{d}y]$ (relative to the datum) is $f(y)\,\mathrm{d}y$. They also used the exceedance probability $F(y) = \int_y^\infty f(z)\,\mathrm{d}z$. The average thickness L of the bed above a certain level y is defined by the conditional mean:

$$L(y) = \int_y^\infty (z - y)f(z)\,\mathrm{d}z \qquad (30)$$

whose integration by parts gives $L(y) = \int_y^\infty F(z)\,\mathrm{d}z$. They then considered an infinitesimal control volume of length $\mathrm{d}x$ and height $\mathrm{d}y$. This volume's contribution to the mean thickness L is $|\mathrm{d}L| = F(y)\,\mathrm{d}y$. Mass conservation (in the spirit of the Exner equation) implies that:

$$\frac{\partial}{\partial t}((1-\zeta)F(y)\,\mathrm{d}x\,\mathrm{d}y) = (D_e - E_e)\,\mathrm{d}x\,\mathrm{d}y \qquad (31)$$

where D_e and E_e are the elevation-specific densities of deposition and entrainment. The authors assumed that although the mean bed level $y_b(t)$ varied slowly with time, the bed elevation's probability density function $f(y)$ was unaffected by that variation. They then made a change of variable $y = \xi + y_b(t)$, where ξ is the bed elevation fluctuation relative to the mean bed level y_b. This linear change of variable implies that the probability density function f_ξ is $f_\xi(\xi) = f(y)$, and by using the chain rule $\partial_t f = (\partial_t \xi)\partial_\xi f$, Parker et al. (2000) turned the mass balance Eq. (31) into:

$$(1 - \zeta_b)f_\xi(\xi)\frac{\partial y_b}{\partial t} = D_e - E_e \qquad (32)$$

which is called the probabilistic formulation of the Exner equation. Integrating Eq. (32) over all bed elevations leads to the classic Exner Eq. (27).

The probabilistic formulation of the Exner equation subsequently became the cornerstone of several morphodynamic models. Astrid Blom and her co-workers combined the probabilistic Exner Eq. (32) and Einstein's definition Eq. (23) of bedload transport rate to study dune migration in non-uniform sediment (Blom, 2008; Blom, Ribberink, & Parker, 2008). Anna Pelosi, Zi Wu and their co-workers were interested in determining the dispersion of randomly entrained tracers buried in the bed (Pelosi, Schumer, Parker, & Ferguson, 2016; Wu et al., 2019).

4.2 *Charru's model (2004)*

Charru et al. (2004) and Charru (2006) developed an empirical model based on the mass conservation of moving particles:

$$\frac{\partial \gamma}{\partial t} + \frac{\partial}{\partial x}(\gamma \bar{u}_p) = E - D \qquad (33)$$

The Exner Eq. (27) and Eq. (33) are equivalent when $\partial_t \gamma \approx 0$ (Ancey & Heyman, 2014). Charru et al. (2004) assumed that the

deposition rate D was proportional to the rate at which particles hit the bed, and the entrainment rate E was considered to depend on the Shields number Θ:

$$D \propto \frac{\gamma}{t_s} \text{ and } E \propto \frac{d}{t_s}f(\Theta - \Theta_c) \qquad (34)$$

where $t_s = d/v_s$ is a time related to the settling velocity $v_s = ((\rho_s - \rho)gd/\rho)^{1/2}$ (for turbulent flows), and f is a function of the difference between the Shields number Θ and its critical value Θ_c. Experiments suggest that f is a linear function of its argument (Charru et al., 2004; Lajeunesse, Malverti, & Charru, 2010) and that the mean particle velocity can be expressed as:

$$\bar{u}_p = v_s(a(\sqrt{\Theta} - \sqrt{\Theta_c}) + b) \qquad (35)$$

where a and b are two constants (Lajeunesse et al., 2010). The bedload transport rate is defined from the particle activity (Section 2.3):

$$q_s = \gamma \bar{u}_p \qquad (36)$$

and thus, under steady-state conditions for flat beds at equilibrium, γ is constant, deposition and entrainment rates match each other (that is, $D = E$), and thus the particle activity is proportional to the stress difference:

$$\gamma \propto d(\Theta - \Theta_c) \qquad (37)$$

which leads to the bedload transport rate:

$$q_{s,eq} = \gamma \bar{u}_p \propto dv_s(\Theta - \Theta_c)(a(\sqrt{\Theta} - \sqrt{\Theta_c}) + b) \qquad (38)$$

This provides a scaling $q_s \propto (\Theta - \Theta_c)$ in the limit $\Theta \to \Theta_c$, and $\Theta^{3/2}$ for $\Theta \gg \Theta_c$.

Under low-to-moderate sediment transport conditions, the bed does not remain flat, but develops bedforms. Under steady-state conditions, Charru et al. (2004) cast the mass balance equation in the following form:

$$l_d \frac{\partial}{\partial x}(\gamma \bar{u}_p) = q_{s,eq} - q_s \qquad (39)$$

where $l_d = t_s \bar{u}_p$ is the mean deposition length, that is, the mean length travelled by a saltating particle between two bounces. This equation shows that the bedload transport rate adjusts to local variations in the bed topography over the distance l_d, called the relaxation or saturation length. As the bedload transport rate satisfies a relaxation equation, there is no one-to-one relationship between q_s and the flow variables ($\bar{u}$ and h), and this relaxation produces an effect similar to the phase lag in bottom shear stress, which is considered to be a key element enabling the Saint-Venant–Exner equations to generate bed instabilities (Section 3.2). Therefore, using Eq. (39) jointly with the Saint-Venant–Exner equations (25)–(27) makes it possible to obtain the desired condition of bed instability (Andreotti, Claudin,

Devauchelle, Durán, & Fourrière, 2012; Charru, 2006; Fourrière et al., 2010). Furthermore, the relaxation length l_d acts as a cut-off length that stabilizes the shortest wavelengths (Andreotti et al., 2012), that is, the generated ripple length scales with l_d in close agreement with experiments.

4.3 *Ancey's model (2008)*

Intrigued by the existence of wide (non-Gaussian) fluctuations in bedload transport rates, Ancey et al. (2006) first tried to see how Einstein's framework could be extended to generate wide, non-Gaussian fluctuations. By considering that the alternation between states of rest and movement experienced by N particles is equivalent to the sum of N telegrapher's processes, they showed that the number of moving particles followed a binomial distribution. Therefore, in the limit of large N, the particle activity probability distribution comes close to the Gaussian distribution. They concluded that something was amiss in this Einsteinian framework: in the absence of positive feedback that exacerbated fluctuations, particle activity and bedload transport did not exhibit large fluctuations.

Ancey, Davison, Böhm, Jodeau, and Frey (2008) adopted a different view to resolve this problem: they considered a fixed control volume and counted the number of moving particles N. This number varies as particles are entrained, deposited, leave or enter the control volume. To quantify these variations, they used birth–death–emigration–immigration Markov processes to calculate the probability $P(n, t)$ of observing $N = n$ particles moving in the control volume at time t. Such processes are classed as stochastic jump processes, and thus are based on two fundamental assumptions: the process is Markovian if the probability $P(n, t)$ depends only on the system state at time $t - \delta t$ (with δt being a short time increment) and not on the whole history up to time t, and it is a jump random process if N varies by 1, 0 or -1 during time step δt. In other words, a single event can occur within time step δt, which eliminates the possibility of coherent particle motion in the form of sediment waves. The assumptions seem reasonable, at least at low bedload transport rates, and they make it possible to use the machinery of random jump processes, notably its analytical tools.

Ancey et al. (2008) assumed that within time step δt, the (transition) probability that a particle would be entrained was $P(n \to n+1; \delta t) = (\lambda + \mu n)\delta t$, where λ and μ are two entrainment parameters. This equation introduces the desired positive feedback: a particle can be entrained from the bed at a rate λ, reflecting the erosive action of the stream, or it can be entrained because it is destabilized by moving particles (due to collisions, increased turbulence, etc.). The latter process occurs at a rate μn proportional to the number of moving particles. Moving particles can be deposited at a probability σn or leave the control volume with a probability $\nu_{out} n$. In both cases the transition probabilies are proportional to n. Particles enter the control volume at a rate ν_{in}. Ancey et al. (2008) showed that the probability $P(N = n, t)$ satisfied a partial differential

equation (called a *master equation*) which admitted steady-state solutions. When the entrainment parameter μ is non-zero, the steady-state solution is the negative binomial distribution:

$$P(N = n) = \frac{\Gamma(r + n)}{\Gamma(r)n!} p^r (1 - p)^n \qquad (40)$$

with $r = (\lambda + \nu_{in})/\mu$ and $p = 1 - \mu/(\nu_{out} + \sigma)$. Equation (40) has been found to agree well with experimental data (Ancey et al., 2008).

The next step is to pass from a discrete formulation in a control volume of length δx to a continuum description valid for $\delta x \to 0$. Ancey and Heyman (2014) defined the continuous random variable:

$$c = \lim_{\delta x \to 0} \frac{N}{\delta x} \qquad (41)$$

which is nothing but the instantaneous (random) particle activity expressed in terms of the number density of moving particles rather than their volume per unit of streambed area. The problem is how to determine the governing equation for the continuous variable c when the only equation available is the master equation describing the changes in the discrete variable N. Ancey and Heyman (2014) used a technique called the Poisson representation, which can be seen as a kind of Laplace or Fourier transform for mapping continuous and discrete probability spaces. They eventually showed that the Poisson density $b(x, t)$ – the image of c in the Poisson space – satisfied a stochastic advection equation:

$$\frac{\partial}{\partial t} b + \frac{\partial}{\partial x} (\bar{u}_p b) = \lambda_d - (\sigma - \mu) b + \sqrt{2\mu b}\, \xi_b \qquad (42)$$

where $\lambda_d = \lim_{\delta x \to 0} \lambda/\delta x$ and ξ_b is a white noise term uncorrelated in time and space. When particle velocity is constant, taking the ensemble average of Eq. (42) leads to a deterministic advection equation for the mean particle activity $\gamma = \bar{\omega}_p \langle c \rangle$ (where $\bar{\omega}_p$ denotes the particle volume per unit streambed width):

$$\frac{\partial}{\partial t} \gamma + \frac{\partial}{\partial x} (\bar{u}_p \gamma) = \lambda' - (\sigma - \mu) \gamma \qquad (43)$$

with $\lambda' = \bar{\omega}_p \lambda_d$. The derivation seems complicated for a result that looks simple, yet a few subtle points should be noted. Equation (43) is valid in the limit of $\delta x \to 0$. In many applications, Eq. (43) is used in a discretized form (for instance, when solving it numerically). In that case, spatial correlations cannot be ignored when taking the ensemble average of Eq. (42). Ancey, Bohorquez, and Heyman (2015) showed that these correlations add a diffusive-like term (the term is not strictly diffusive, but behaves like linear diffusion), and Eq. (43) could be approximated by an advection–diffusion equation:

$$\frac{\partial}{\partial t} \gamma + \frac{\partial}{\partial x} (\bar{u}_p \gamma) = \lambda' - (\sigma - \mu) \gamma + \frac{\partial^2}{\partial x^2} (D_* \gamma) \qquad (44)$$

where $D_* = \bar{u}_p \Delta x / 2$ is a pseudo diffusion factor (diffusivity). This shows that even when particles move at constant velocity, the time variations in particle activity are described by an advection–diffusion equation whose diffusivity is scale dependent. When particles move with varying velocity, velocity fluctuations add further diffusion, but the governing equation remains structurally identical to Eq. (44). In that case, the mean particle transport rate can be defined as:

$$\langle q_s \rangle = \gamma \bar{u}_p - \frac{\partial}{\partial x}(D_u \gamma) \qquad (45)$$

where D_u is the particle diffusivity including the effects of particle velocity fluctuations and spatial correlation. This form is identical to that found by Furbish, Haff, et al. (2012) using a different approach (Section 4.4). Equation (44) can be recast in the form:

$$\frac{\partial \langle q_s \rangle}{\partial x} = E - D - \frac{\partial \gamma}{\partial t} \qquad (46)$$

where $E = \lambda' + \mu \gamma$ and $D = \sigma \gamma$ are the entrainment and deposition rates. We retrieve the commonest form of Exner Eq. (27) when $\partial_t \gamma$ can be neglected. As with Charru's model (Section 4.2), the transport rate is not a one-to-one function of the flow variables, and thus the Saint-Venant–Exner equations are unstable, even for $\mathsf{F} < 2$ (Bohorquez & Ancey, 2015).

4.4   *Furbish's model (2012)*

David Furbish and his co-workers took inspiration from statistical theories of gas dynamics to provide a probabilistic description of bedload transport (under rarefied transport conditions) and consistency rules. One of their key results was the definition of the mean bedload transport rate (Furbish, Childs, Haff, & Schmeeckle, 2009; Furbish, Haff, et al., 2012; Furbish, Fathel, Schmeeckle, Jerolmack, & Schumer, 2017). A qualitative assessment can be obtained as follows. Let us define the local transport rate as:

$$q_s = \gamma u_p \qquad (47)$$

where γ is the local particle activity and u_p is the particle velocity. Taking the ensemble average and using the Reynolds decomposition rule, we get:

$$\langle q_s \rangle = \langle \gamma \rangle \langle u_p \rangle + \langle \gamma' u_p' \rangle \qquad (48)$$

where γ' and u_p' are the fluctuating contributions, and the brackets $\langle \rangle$ represent the ensemble average (that is, a statistical average over all possible configurations). As with turbulence, the goal is to find a closure equation for the fluctuating component $\langle \gamma' u_p' \rangle$. Furbish, Haff, et al. (2012) showed that the fluctuating term $\langle \gamma' u_p' \rangle$ reflected particle diffusion and could be closely approximated by $-\partial_x(D_r \langle \gamma \rangle)$. Thus, the bedload transport rate

can be expressed as:

$$\langle q_s \rangle = \langle \gamma \rangle \langle u_p \rangle - \frac{\partial}{\partial x}(D_r \langle \gamma \rangle) \qquad (49)$$

where D_r is the particle diffusivity:

$$D_r(x, t) = \lim_{dt \to 0} \frac{1}{2dt} \int_{-\infty}^{+\infty} r^2 f_r(x + r, t + dt \,|\, x, t) \, dr \qquad (50)$$

Equation (49) can be derived more rigorously. Furbish, Haff, et al. (2012) used the Chapman–Kolmogorov equation representing the mass conservation of moving particles in probabilistic terms. This is a general equation ensuring the consistency of the motion; it deduces the probability of finding a particle at position x at time $t + \delta t$ from all the possible positions that this particle could have occupied at time t:

$$f_x(x, t + \delta t) = \int_{-\infty}^{+\infty} f_x(x - r, t) f_r(r, \delta t | x - r, t) \, dr \qquad (51)$$

where $f_x(x, t)$ is the probability density function of finding a particle at x at time t and $f_r(r; x, t)$ is the jump probability, that is, the probability density function of observing a particle jumping by r within length of time δt, passing from $x - r$ at time t to x at time $t + \delta t$. Under certain conditions of continuity, this equation is equivalent to a partial differential equation called the Fokker–Planck equation:

$$\frac{\partial}{\partial t} f_x + \frac{\partial}{\partial x}(\bar{u}_p f_x) = \frac{\partial^2}{\partial x^2}(D_r f_x) \qquad (52)$$

From this general equation, Furbish, Haff, et al. (2012) deduced the definition of the bedload transport rate Eq. (49).

The important point, underscored by Furbish, Fathel, et al. (2017), is that the mean bedload transport rate is not uniquely determined: $\langle q_s \rangle$ is not only a local function of particle activity γ and particle velocity u_p but it also varies because of the gradient of particle activity $-\partial_x(D_r \langle \gamma \rangle)$, reflecting a non-local behaviour. It has often been advocated that non-locality is the hallmark of anomalous diffusion and heavy-tailed distribution f_r (Foufoula-Georgiou, Ganti, & Dietrich, 2010; Ganti et al., 2010; Voller & Paola, 2010). This is not the case here, however, as the statistical treatment only considers active (moving) particles, whereas in studies of tracer particles motion alternates with phases of rest and burial, and this makes the statistical analysis far more complicated (Section 5.3).

Furbish, Haff, et al. (2012) and Furbish, Fathel, et al. (2017) also derived another useful definition of the mean bedload transport rate. Using the Eq. (29) definition of q_s in the entrainment form of the Exner equation and a Fokker–Planck approximation

of the integral term, they found that:

$$\langle q_s \rangle = E \langle l \rangle - \frac{\partial}{\partial x}(E \langle l^2 \rangle) \qquad (53)$$

where $\langle l \rangle$ denotes the mean hop length and $\langle l^2 \rangle$ is its second-order moment. The first contribution to the right-hand side is nothing other than the definition Eq. (23) used by Einstein (1950) to compute the transport rate under steady-state conditions. The second contribution reflects non-local effects when entrainment is non-homogeneous along the bed. The strict equivalence of forms Eq. (53) and Eq. (49) may ultimately reconcile Einstein's and Kalinske's approaches. Indeed, Kalinske questioned Einstein's definition of q_s as it did not include any information on particle velocity (Einstein, 1942; Kalinske, 1947).

5 Lagrangian and particle-dynamics models

5.1 *Isolated particles*

In the wake of Kalinske's and Bagnold's works (Sections 2.3 and § 2.1, respectively), models have tried to determine the bedload transport rate q_s from the mean behaviour of the particles (Ali & Dey, 2019). This approach has been gradually abandoned. Indeed, Seminara et al. (2002) showed that Bagnold's assumption was flawed. Furthermore, there is growing evidence that bedload transport rate fluctuations arise mainly from variations in particle activity rather than the mean particle velocity (Ancey et al., 2008; Heyman et al., 2016).

5.2 *The collective motion of particles*

By the late 1970s, a renewal of interest in granular flow theory had led to recognition of the importance of velocity fluctuations in stress generation (Haff, 1983; Savage, 1984). Rapid granular flows were viewed as granular gases. Inelastic collisions give rise to velocity fluctuations at the particle scale, and at the bulk scale they generate the pressure p and shear stress τ that are related to the degree of particle agitation (quantified through their thermal velocity $v = \sqrt{T}$ or granular temperature $T = (1/n)\langle u_i'^2 \rangle$, where u_i' are the fluctuating velocity components and n is the space dimension). Pressure $p = \rho_p f_1(T, e, \phi)T$ and shear stress $\tau = \rho_p d f_2(T, e, \phi)\sqrt{T}\dot{\gamma}$, where f_1 and f_2 are two constitutive functions of the granular temperature T and the particle elasticity e, ϕ is the solid volume fraction, and $\dot{\gamma}$ denotes the shear rate. Intense sediment transport can also be modelled as a granular gas, and thus it is a natural candidate for an application of kinetic theory (Jenkins & Hanes, 1998).

Under steady-state uniform-flow conditions, this approach leads to the momentum balance equations for the particle flow:

$$\phi \rho_p g \sin\theta + \frac{d\tau}{dy} + f_i(u_p, u_f) = 0 \qquad (54)$$

$$-\phi \rho_p g \cos\theta - \frac{dp}{dy} = 0 \qquad (55)$$

and for the water flow:

$$(1 - \phi)\rho_f g \sin\theta + \frac{d\tau_f}{dy} - f_i(u_p, u_f) = 0 \qquad (56)$$

$$-(1 - \phi)\rho_f g \cos\theta - (1 - \phi)\frac{dp_f}{dy} = 0 \qquad (57)$$

where u_f, τ_f and p_f denote the fluid velocity, shear stress and pressure, respectively, and f_i is the interaction stress between the solid and fluid phases. Various constitutive equations have been proposed to close these systems of Eqs (54)–(57), starting with simple equations – where a viscous drag force is considered for the interaction stress f_i, and kinetic theory is considered for the collisional stresses p and τ (Jenkins & Hanes, 1998) – and moving to refined models taking various processes into account, such as the effect of collisions on fluid turbulence (Capart & Fraccarollo, 2011). The mass and momentum balance equations must be supplemented by the boundary conditions that specify how granular temperature is generated along the bed. Because of the high degree of nonlinearity in the resulting governing equations, there are no analytical solutions to Eqs (54)–(56). Approximate solutions can be obtained by fitting power-law functions to the numerical solutions of Eqs (54)–(57). For instance, Hsu, Jenkins, and Liu (2004) found that the dimensionless equation:

$$\Phi = 20.0(\Theta - \Theta_c)^{1.8} \qquad (58)$$

closely matched their numerical solutions (with $\Theta_c \sim 0.05$ the dimensionless critical stress), whereas Capart and Fraccarollo (2011) found that the mean bedload transport rate scales as $\Phi \approx 4.2\Theta^{3/2}$ for $\Theta \leq 3$. Although these two scalings bear some resemblance with the MPM Eq. (5), we note that the proportionality factor is quite different.

One longstanding issue in granular flow theory has concerned the calculation of the stresses generated by sustained frictional contacts within the network of moving particles. The empirical approach known as "$\mu(I)$ rheology" was developed to that end; it met with considerable success in dry granular flows (Forterre & Pouliquen, 2008) and has been extended to bedload transport (Armanini, Larcher, Nucci, & Dumbser, 2014; Berzi & Jenkins, 2008; Maurin, Chauchat, & Frey, 2016; Revil-Baudard & Chauchat, 2013). These models usually show that the mean bedload transport rate q_s scales as $(\Theta - \Theta_c)^{3/2}$ in accordance with the MPM Eq. (5), but as the incipient motion phase (that is, when $\Theta \to \Theta_c$) corresponds to rarefied flow conditions for which the continuum assumption may break down, they may be inaccurately describing this phase. Ever better numerical simulations have enabled discrete element methods (DEM) to be coupled with continuum hydrodynamic models of the fluid phase, thus making it possible to avoid the continuum

assumption for the particle flow. For instance, within this frame-work, Pähtz and Durán (2018) found that particle activity scales as $\gamma \propto \Theta - \Theta_c$ and that the scaling $\Psi \propto (\Theta - \Theta_c)^{3/2}$ roughly captures their numerical data.

5.3   *Statistical behaviour*

Since Einstein (1937), marked particles (tracers) have com-monly been used for studying bedload transport in the field (Bradley & Tucker, 2012; Cassel, Dépret, & Piégay, 2017; Drake, 1988; Ferguson et al., 2002; Haschenburger, 2013; Has-san, Church, & Schick, 1991; Liébault, Bellot, Chapuis, Klotz, & Deschâtres, 2012; Olinde & Johnson, 2015). Measuring the displacements of a set of tagged particles over a given time makes it possible to deduce their virtual velocity, the entrainment rate and the bedload transport rate (Wilcock, 1997) (Section 3.1). The theoretical problem of particle dispersion has long been a central one when using fluid mechanics to study tur-bulent shear flows, Brownian motion and viscous suspension. A standard tool created to study the erratic motion of Brownian particles is the variance of the particle displacement r. Let us assume that between times t and $t + \tau$, the particle has moved by $r(\tau) = x(t + \tau) - x(t)$. The ensemble average $\langle r \rangle$ gives us information on the particle velocity ($\langle r \rangle = u_p \tau$ for short times τ), whereas the variance:

$$R(\tau) = \langle (r - \langle r \rangle)^2 \rangle \tag{59}$$

tells us how far the particle can move away from its average position. For a Brownian particle experiencing molecular colli-sions in water, this variance increases linearly with time: $R(\tau) = 2D\tau$, where D is called the diffusion constant (or diffusivity). This case is called *normal* Fickian or Brownian diffusion. Yet, at very short timescales (that is, a few nanoseconds), water is a strongly correlated medium, and Brownian particles exhibit micro-displacements which lead to a quadratic time variation: $R \propto \tau^2$. This regime is called *ballistic* (Mo & Raizen, 2019).

Using numerical simulations and field data, Nikora, Heald, Goring, and McEwan (2001) and Nikora, Habersack, Huber, and McEwan (2002) suggested that similarly to Brownian motion, bedload particles exhibit different diffusion regimes, which can be distinguished depending on the value of the exponent α:

$$R(\tau) \propto \tau^\alpha \tag{60}$$

with $\alpha \sim 2$ at short times (ballistic regime for saltating par-ticles during their flights), $\alpha \sim 1$ at intermediate timescales (normal diffusion) and $\alpha < 1$ at long timescales (global regime featuring subdiffusion and resulting from motion intermittency during the rest and burial phases). They also suggested that the transition from the normal to the global regime occurred at timescales $T \sim 15u_* d$. The existence of the ballistic and normal-diffusion regimes has been thoroughly confirmed (Bradley, Tucker, & Benson, 2010; Cecchetto et al., 2018; Fathel, Furbish,

& Schmeeckle, 2015; Furbish, Ball, & Schmeeckle, 2012; Furbish, Fathel, et al., 2017; Martin, Jerolmack, & Schumer, 2012; Heyman et al., 2016) even though additional issues (particle sorting, censored data) blur the picture. The subdiffu-sive behaviour of tracers has also been shown in field survey data (Nikora et al., 2002; Zhang, Meerschaert, & Packman, 2012). The mechanisms underlying the subdiffusive regime have attracted growing attention in recent years. A suitable framework has been offered by random-walk theory (Schumer et al., 2009; Zhang et al., 2012). Let us assume that at discrete time:

$$t_{n+1} = t_n + \delta t_n \tag{61}$$

where δt_n is the waiting time between two events, the particle moves from x_n to:

$$x_{n+1} = x_n + \delta x_n \tag{62}$$

where δx_n is the hop length. When both the waiting time δt_n and hop length δx_n are independent, identically distributed ran-dom variables with finite mean and variance, the central limit theorem enables an approximation of the total displacement $\sum_i \delta x_i \approx \bar{u}_p t + D_r \sqrt{t} \varepsilon$ (with ε a normal random number) and time $\sum_i \delta t_i$ (Schumer et al., 2009). The consequence is that the particle activity γ satisfies an advection–diffusion equation:

$$\frac{\partial}{\partial t} \gamma + \bar{u}_p \frac{\partial}{\partial x} \gamma = D_r \frac{\partial^2}{\partial x^2} \gamma \tag{63}$$

When the waiting time and/or hop length do not have finite means, it can be shown that the particle activity γ satisfies a fractional advection–diffusion equation:

$$\frac{\partial^\alpha}{\partial t} \gamma + \bar{u}_p \frac{\partial}{\partial x} \gamma = D_r \frac{\partial^\beta}{\partial x^\beta} \gamma \tag{64}$$

Fractional diffusion is a growing field of study in physics. It is a promising line of research with regards to non-locality, long-term memory and fractal properties. Based on the integration and differentiation of non-integer orders (the fractional calcu-lus), it requires special numerical methods for solving equations, which are more difficult to implement than those used for normal diffusion (Schumer et al., 2009).

6   Concluding remarks

This paper has provided a historical overview of the approaches used for bedload transport modelling. It has outlined efforts made since the 2000s to gain new physical insights into bedload transport rates and to improve prediction. These efforts certainly hold promise, but no decisive breakthrough in the computation of bedload transport rates has been accomplished since then, nor is expected in the medium term. Chris Paola summarizes the current situation: "I find it remarkable that we can (evidently) calculate the quantum states of an electron to much greater

accuracy than we can calculate the flow rate of sand grains in a stream" (C. Paola, personal communication). So, what is so complicated about bedload transport? Are we currently bumping against a ceiling or are we at the limits of predictability? In a system in which everything fluctuates over time, does this limit stem from the large degree of freedom of natural systems?

It is not all doom and gloom, however. There is not a shred of evidence that the absence of significant progress means the failure of accurate quantitative methods (although the reverse is also true). There are many reasons why bedload transport is difficult to predict: the mix of fast and slow processes, non-equilibrium and noise-driven processes, cascades of interacting processes, the varying temporal and spatial scales dependent on flow conditions, the heterogeneity of materials and flow conditions, nonlinearity, threshold effects, hysteresis, poor knowledge of initial and boundary conditions, scale effects between laboratory and field conditions, difficulties in obtaining reliable measurements, human action, and so on. Bedload transport is no exception to the rule that prediction is difficult, but not impossible, in complex systems, although the meaning of predictability and the tolerance to error have to be defined accurately (Mitchell, 2009). In comparison with other fields marked by "complexity", the future of bedload transport modelling has some advantages: (i) measurements and direct observations are possible; (ii) holistic and reductionist approaches have been developed (e.g. see the Socratic dialogue in Seminara & Bolla Pittaluga, 2012); and (iii) the field does not suffer from the over-specialization and compartmentalization of its research activities, with river restoration as a case in point (Smith, Clifford, & Mant, 2014; Wohl et al., 2005).

In the present manuscript's companion paper (Ancey, 2020), I outline some future prospects for the field; I also return to the question of why progress is currently so slow.

Funding

Supplemental data

Notation

a	=	material coefficient (s^2/m^{-1})
c	=	bed wave speed (m s^{-1})
c_l	=	lift coefficient (–)
d	=	mean particle diameter (m)
D	=	deposition rate (kg s^{-1})
D_*	=	pseudo diffusion factor (diffusivity) ($= \bar{u}_p \, \Delta x / 2$) (m^2 s^{-1})
D_r	=	particle diffusivity (m^2 s^{-1})
e	=	particle elasticity (–)
e_b	=	bedload transport efficiency factor (–)
E	=	entrainment rate (kg s^{-1})
F	=	Froude number (–)
g	=	gravitational acceleration (m s^{-2})
$h(x,t)$	=	flow depth (m)
H	=	phase-indicating function (–)
i	=	bed slope (–)
$\bar{l}$	=	leap length (m)
L_a	=	layer thickness (m)
n	=	number of particles (–)
$\boldsymbol{n}$	=	unit normal to the control surface
p_f	=	pressure (Pa)
q_c	=	critical discharge (kg m^{-1} s^{-1})
q_s	=	bedload transport rate per unit width (kg m^{-1} s^{-1})
$\bar{q}_s$	=	mean transport rate (kg m^{-1} s^{-1})
q_w	=	water discharge per unit width (kg m^{-1} s^{-1})
Q_s	=	bedload transport rate (kg s^{-1})
R	=	density ratio ($= \rho_s/\rho - 1$)
t_e	=	exchange time (s)
T	=	granular temperature (kg m^2 s^{-2})
u	=	fluid velocity at the grain level (m s^{-1})
u_*	=	friction velocity ($= \sqrt{\tau_b/\rho}$) (m s^{-1})
u_c	=	critical fluid velocity (m s^{-1})
u_f	=	fluid velocity (m s^{-1})
u_i'	=	fluctuating velocity components (m s^{-1})
$\bar{u}$	=	depth-averaged water velocity (m s^{-1})
$\bar{u}_p$	=	mean velocity of particles (m s^{-1})
U_p	=	virtual velocity (m s^{-1})
v	=	thermal velocity (m s^{-1})
V	=	migration celerity (m s^{-1})
x	=	downstream position (m)
$y_b(x,t)$	=	bed elevation (m)
α	=	dynamic friction coefficient (–)
γ	=	particle activity (m)
$\dot{\gamma}$	=	shear rate (s^{-1})
δ	=	height scale (m)
ζ	=	bed porosity (−)
θ	=	bed inclination (−)
Θ_c^*	=	dimensional critical shear stress ($= 0.047$)
ν	=	eddy viscosity (kg s^{-1} m^{-1})
ξ	=	bed elevation fluctuation relative to the mean bed level y_b (m)
ρ	=	water density (kg m^{-3})
ρ_s	=	sediment density (kg m^{-3})
τ_b	=	bottom shear stress (Pa)
τ_c	=	critical shear stress (Pa)
τ_f	=	shear stress (Pa)
ϕ	=	solid volume fraction (–)
Φ	=	dimensionless bedload transport rate (–)
χ_*	=	material coefficient (s^2 m^{-1})

Ψ =   flow intensity (–)
ω =   stream power ($\text{kg m}^2 \text{s}^{-3}$)

References

Ali, S. Z., & Dey, S. (2019). Bed particle saltation in turbulent wall-shear flow: A review. *Proceedings of the Royal Society of London Series A*, *475*, 20180824.

Ancey, C. (2020). Bedload transport: a walk between randomness and determinism. Part 2. Challenges and prospects. *Journal of Hydraulic Research*. doi:10.1080/00221686.2019.1702595

Ancey, C., Bigillon, F., Frey, P., & Ducret, R. (2003). Rolling motion of a single bead in a rapid shallow water stream down a steep channel. *Physical Review E*, *67*, 011303.

Ancey, C., Böhm, T., Jodeau, M., & Frey, P. (2006). Statistical description of sediment transport experiments. *Physical Review E*, *74*, 011302.

Ancey, C., Bohorquez, P., & Heyman, J. (2015). Stochastic interpretation of the advection diffusion equation and its relevance to bed load transport. *Journal of Geophysical Research. Earth Surface*, *120*, 2529–2551.

Ancey, C., Davison, A. C., Böhm, T., Jodeau, M., & Frey, P. (2008). Entrainment and motion of coarse particles in a shallow water stream down a steep slope. *Journal of Fluid Mechanics*, *595*, 83–114.

Ancey, C., & Heyman, J. (2014). A microstructural approach to bed load transport: mean behaviour and fluctuations of particle transport rates. *Journal of Fluid Mechanics*, *744*, 129–168.

Andreotti, B., Claudin, P., Devauchelle, O., Durán, O., & Fourrière, A. (2012). Bedforms in a turbulent stream: ripples, chevrons and antidunes. *Journal of Fluid Mechanics*, *690*, 94–128.

Armanini, A. (2018). *Principles of river hydraulics*. Berlin: Springer.

Armanini, A., Cavedon, V., & Righetti, M. (2014). A probabilistic/deterministic approach for the prediction of the sediment transport rate. *Advances in Water Resources*, *81*, 10–18.

Armanini, A., Larcher, M., Nucci, E., & Dumbser, M. (2014). Submerged granular channel flows driven by gravity. *Advances in Water Resources*, *63*, 1–10.

Bagnold, R. (1956). The flow of cohesionless grains in fluids. *Proc. R. Soc. London*, *249*, 235–296.

Bagnold, R. A. (1980). An empirical correlation of bedload transport rates in flumes and natural rivers. *Proceedings of the Royal Society of London Series A*, *372*, 453–473.

Bagnold, R. A. (1986). Transport of solids by natural water flow: evidence for a worldwide correlation. *Proceedings of the Royal Society of London Series A*, *405*, 369–374.

Bailard, J. A., & Inman, D. L. (1979). A reexamination of Bagnold's Granular-fluid model and bed load transport equation. *Journal of Geophysical Research*, *84*, 7827–33.

Ballio, F., Nikora, V., & Coleman, S. E. (2014). On the definition of solid discharge in hydro-environment research and applications. *Journal of Hydraulic Research*, *52*, 173–184.

Ballio, F., Pokrajac, D., Radice, A., & Hosseini Sadabadi, S. A. (2018). Lagrangian and Eulerian description of bed-load transport. *Journal of Geophysical Research. Earth Surface*, *123*, 384–408.

Balmforth, N., & Provenzale, A. (2001). Patterns of dirt. In N. Balmforth & A. Provenzale (Eds.), *Geomorphological fluid mechanics* (pp. 369–393). Berlin: Springer Verlag.

Berzi, D., & Jenkins, J. T. (2008). A theoretical analysis of free-surface flows of granular-liquid mixtures. *Journal of Fluid Mechanics*, *608*, 393–410.

Blom, A. (2008). Different approaches to handling vertical and streamwise sorting in modeling river morphodynamics. *Water Resources Research*, *44*, W03415.

Blom, A., Ribberink, J., & Parker, G. (2008). Vertical sorting and the morphodynamics of bed form-dominated rivers: A sorting evolution model. *Journal of Geophysical Research*, *113*, F01019.

Blondeaux, P., Colombini, M., Seminara, G., & Vittori, G. (2018). *Introduction to morphodynamics of sedimentary patterns*. Genova: Genova University Press.

Bohorquez, P., & Ancey, C. (2015). Stochastic-deterministic modeling of bed load transport in shallow waterflow over erodible slope: Linear stability analysis and numerical simulation. *Advances in Water Resources*, *83*, 36–54.

Bohorquez, P., Cañada Pereira, P., Jimenez-Ruiz, P. J., & J. D. del Moral-Erencia (2019). The fascination of a shallow-water theory for the formation of megaflood-scale dunes and antidunes. *Earth-Science Reviews*, *193*, 91–108.

Bradley, D. N., & Tucker, G. E. (2012). Measuring gravel transport and dispersion in a mountain river using passive radio tracers. *Earth Surface Processes and Landforms*, *37*, 1034–1045.

Bradley, D. N., Tucker, G. E., & Benson, D. A. (2010). Fractional dispersion in a sand bed river. *Journal of Geophysical Research. Earth Surface*, *115*, F00A09.

Campagnol, J., Radice, A., & Ballio, F. (2012). Scale-based statistical analysis of sediment fluxes. *Acta Geophysica*, *60*, 1744–1777.

Capart, H., & Fraccarollo, L. (2011). Transport layer structure in intense bed-load. *Geophysical Research Letters*, *38*, L20402.

Cassel, M., Dépret, T., & Piégay, H. (2017). Assessment of a new solution for tracking pebbles in rivers based on active RFID. *Earth Surface Processes and Landforms*, *42*, 1938–1951.

Cecchetto, M., Tregnaghi, M., Bottacin-Busolin, A., Tait, S., Cotterle, L., & Marion, A. (2018). Diffusive regimes of the motion of bed-load particles in open channel flows at low transport stages. *Water Resources Research*, *54*, 8674–8691.

Charru, F. (2006). Selection of the ripple length on a granular bed sheared by a liquid flow. *Physics of Fluids*, *18*, 121508.

Charru, F., Mouilleron, H., & Eiff, O. (2004). Erosion and deposition of particles on a bed sheared by a viscous flow. *Journal of Fluid Mechanics*, *519*, 55–80.

Church, M., & Haschenburger, J. K. (2017). What is the "active layer"? *Water Resources Research*, *53*, 5–10.

Coleman, S. E., & Melville, B. W. (1994). Bed-form development. *Journal of Hydraulic Engineering*, *120*, 544–560.

Coleman, S., & Nikora, V. (2009). Exner equation: A continuum approximation of a discrete granular system. *Water Resources Research*, *45*, W09421.

Coleman, S. E., & Nikora, V. I. (2011). Fluvial dunes: initiation, characterization, flow structure. *Earth Surface Processes and Landforms*, *36*, 39–57.

Colombini, M. (2004). Revisiting the linear theory of sand dune formation. *Journal of Fluid Mechanics*, *502*, 1–16.

Dhont, B., & Ancey, C. (2018). Are bedload transport pulses in gravel-bed rivers created by bar migration or sediment waves. *Geophysical Research Letters*, *45*, 5501–5508.

Drake, T. (1988). *Experimental flows of granular materials* (PhD). California, Los Angeles.

du Boys, P. (1879). Le Rhône et les rivières à lit affouillable – Étude du régime du Rhône et de l'action exercée par les eaux sur un lit à fond de graviers indéfiniment affouillable. *Annales des Ponts et Chaussées*, *49*, 141–95.

Einstein, H. (1937). *Der Geschiebetrieb als Wahrscheinlichkeitproblem (Bedload transport as a probability problem)* ((English translation by W. W. Sayre, in Sedimentation (Symposium to honor H. A. Einstein), edited by H. W. Shen, Fort Collins, Colorado, 1972, C1–C105). Zurich: ETHZ.

Einstein, H. (1942). Formulas for the transportation of bed load. *Transactions of the American Society of Civil Engineers*, *107*, 561–597.

Einstein, H. (1950). *The bed-load function for sediment transportation in open channel flows* (Technical Report No. 1026). United States Department of Agriculture.

Ettema, R., & Mutel, C. (2014). *Hans Albert Einstein—His life as a pioneering engineer*. Reston, VA: American Association of Civil Engineers.

Exner, F. (1925). Ueber die Wechselwirkung zwischen Wasser und Geschiebe in Fluessen. *Sitzungsberichte der kaiserlichen Akademie der Wissenschaften Wien, Abteilung IIa*, *134*, 165–205.

Fathel, S., Furbish, D., & Schmeeckle, M. (2015). An experimental demonstration of ensemble behavior in bed load sediment transport. *Journal of Geophysical Research. Earth Surface*, *120*, 2298–2317.

Ferguson, R., Bloomer, D., Hoey, T., & Werritty, A. (2002). Mobility of river tracer pebbles over different timescales. *Water Resources Research*, *38*, 3-1–3-8. doi:10.1029/2001WR000254.

Fernandez Luque, R., & van Beek, R. (1976). Erosion and transport of bed-load sediment. *Journal of Hydraulic Research*, *14*, 127–144.

Ford, C. (2016). *Natural interests. The contest over environment in modern France*. Cambridge, MA: Harvard University Press.

Forterre, Y., & Pouliquen, O. (2008). Flows of dense granular media. *Annual Review of Fluid Mechanics*, *40*, 1–24.

Foufoula-Georgiou, E., Ganti, V., & Dietrich, W. (2010). A nonlocal theory for sediment transport on hillslopes. *Journal of Geophysical Research*, *115*, F00A1.

Fourrière, A., Claudin, P., & Andreotti, B. (2010). Bedforms in a turbulent stream: formation of ripples by primary linear instability and of dunes by nonlinear pattern coarsening. *Journal of Fluid Mechanics*, *649*, 287–328.

Furbish, D., Ball, A., & Schmeeckle, M. (2012). A probabilistic description of the bed load sediment flux: 4. Fickian diffusion at low transport rates. *Journal of Geophysical Research*, *117*, F03034.

Furbish, D., Childs, E., Haff, P., & Schmeeckle, M. (2009). Rain splash of soil grains as a stochastic advection-dispersion process, with implications for desert plant-soil interactions and land-surface evolution. *Journal of Geophysical Research*, *114*, F00A03.

Furbish, D., Fathel, S. L., & Schmeeckle, M. W. (2017). Particle motions and bedload transport theory: the entrainment forms of the flux and the Exner equation. In D. Tsutsumi & J. B. Laronne (Eds.), *Gravel-bed rivers: Processes and disasters* (pp. 97–120). Chichester: John Wiley & Sons.

Furbish, D., Haff, P., Roseberry, J., & Schmeeckle, M. (2012). A probabilistic description of the bed load sediment flux: 1. Theory. *Journal of Geophysical Research*, *117*, F03031.

Furbish, D. J., Fathel, S. L., Schmeeckle, M. W., Jerolmack, D. J., & Schumer, R. (2017). The elements and richness of particle diffusion during sediment transport at small timescales. *Earth Surface Processes and Landforms*, *42*(1), 214–237.

Ganti, V., Meerschaert, M., Foufoula-Georgiou, E., Viparelli, E., & Parker, G. (2010). Normal and anomalous dispersion of gravel tracer particles in rivers. *Journal of Geophysical Research*, *115*, F00A12.

Gilbert, G. K., & Murphy, E. C. (1914). *The transportation of débris by running water* (Technical report). U.S. Geological Survey Professional Paper vol. 86.

Gomez, B. (1991). Bedload transport. *Earth-Science Reviews*, *31*, 89–132.

Graf, W. (1984). *Hydraulics of sediment transport*. Littleton: Water Resources Publications.

Guala, M., Singh, A., BadHeartBull, N., & Foufoula-Georgiou, E. (2014). Spectral description of migrating bed forms and sediment transport. *Journal of Geophysical Research. Earth Surface*, *119*, 123–137.

Haff, P. K. (1983). Grain flow as a fluid-mechanical phenomenon. *Journal of Fluid Mechanics*, *134*, 401–430.

Hager, W. H. (2005). Du Boys and sediment transport. *Journal of Hydraulic Research*, *43*, 227–233.

Hager, W. H. (2009). *Hydraulicians in Europe 1800–2000*. Boca Raton, FL: CRC Press.

Hager, W. H. (2018). Bed-load transport: advances up to 1945 and outlook into the future. *Journal of Hydraulic Research*, *56*, 596–607.

Hamamori, A. (1962). *A theoretical investigation on the fluctuations of bed load transport* (Technical Report No. R4). Delft Hydraulics Laboratory.

Haschenburger, J. K. (2013). Tracing river gravels: Insights into dispersion from a long-term field experiment. *Geomorphology*, *200*, 121–131.

Hassan, M. A., Church, M., & Schick, A. P. (1991). Distance of movement of coarse particles in gravel bed streams. *Water Resources Research*, *27*, 503–511.

Heyman, J., Bohorquez, P., & Ancey, C. (2016). Entrainment, motion, and deposition of coarse particles transported by water over a sloping mobile bed. *Journal of Geophysical Research. Earth Surface*, *121*, 1931–1952.

Hino, M. (1968). Equilibrium-range spectra of sand waves formed by flowing water. *Journal of Fluid Mechanics*, *34*, 565–573.

Hsu, T.-J., Jenkins, J. T., & Liu, P. L.-F. (2004). On two-phase sediment transport: sheet flow of massive particles. *Proceedings of the Royal Society of London Series A*, *460*, 2223–2250.

James, S. C., Jones, C. A., Grace, M. D., & Roberts, J. D. (2010). Advances in sediment transport modelling. *Journal of Hydraulic Research*, *48*, 754–763.

Jenkins, J. T., & Hanes, D. M. (1998). Collisional sheet flows of sediment driven by a turbulent fluid. *Journal of Fluid Mechanics*, *370*, 29–52.

Kalinske, A. A. (1947). Movement of sediment as bed load in rivers. *Transactions, American Geophysical Union*, *28*, 615–62.

Lajeunesse, E., Malverti, L., & Charru, F. (2010). Bed load transport in turbulent flow at the grain scale: Experiments and modeling. *Journal of Geophysical Research*, *115*, F04001.

Lammers, R. W., & Bledsoe, B. P. (2018). Parsimonious sediment transport equations based on Bagnold's stream power approach. *Earth Surface Processes and Landforms*, *43*, 242–258.

Levi, E. (1995). *The science of water. The foundations of modern hydraulics*. New York, NY: American Association of Civil Engineers.

Liébault, F., Bellot, H., Chapuis, M., Klotz, S., & Deschâtres, M. (2012). Bedload tracing in a high-sediment-load mountain stream. *Earth Surface Processes and Landforms*, *37*, 385–399.

Lisle, I. G., Rose, C. W., Hogarth, W. L., Hairsine, P. B., Sander, G. C., & J.-Y. Parlange (1998). Stochastic sediment transport in soil erosion. *Journal of Hydrology*, *204*, 217–230.

Lisle, T. E. (2004). Sediment wave. In A. Goudie (Ed.), *Encyclopedia of geomorphology* (Vol. 2, pp. 938). London: Routledge.

Martin, R., Jerolmack, D., & Schumer, R. (2012). The physical basis for anomalous diffusion in bed load transport. *Journal of Geophysical Research*, *117*, F01018.

Martin, Y. (2000). Modelling hillslope evolution: linear and nonlinear transport relations. *Geomorphology*, *34*, 1–21.

Maurin, R., Chauchat, J., & Frey, P. (2016). Dense granular flow rheology in turbulent bedload transport. *Journal of Fluid Mechanics*, *804*, 490–512.

Meyer-Peter, E., Favre, H., & Einstein, H. (1934). Neure Versuchsresultate über den Geschiebetrieb. *Schweizerische Bauzeitung*, *113*, 147–150.

Meyer-Peter, E., & Müller, R. (1948). Formulas for bed load transport. In *Proceedings of the 2nd Meeting of the International Association of Hydraulic Structures Research (IAHSR)*, Stockholm, Sweden, 7–9 June 1948 (pp. 39–64).

Mitchell, M. (2009). *Complexity, a guided tour*. New York, NY: Oxford University Press.

Mo, J., & Raizen, M. (2019). Highly resolved brownian motion in space and in time. *Annual Review of Fluid Mechanics*, *51*, 401–428.

Nakagawa, H., & Tsujimoto, T. (1980). Sand bed instability due to bed load motion. *Journal of the Hydraulics Division*, *106*, 2029–2051.

Nikora, V. (1984). *The structure of turbulent flow and statistical characterisation of dune-covered river beds (with examples of field studies in rivers Turunchuk, Rioni, and Tsheniscali)* (Unpublished doctoral dissertation).

Nikora, V., Habersack, H., Huber, T., & McEwan, I. (2002). On bed particle diffusion in gravel bed flows under weak bed load transport. *Water Resources Research*, *38*, WR000513.

Nikora, V., Heald, J., Goring, D., & McEwan, I. (2001). Diffusion of saltating particles in unidirectional water flow over a rough granular bed. *Journal of Physics A: Mathematical and General*, *34*, L743–L749.

Nikora, V. I., Sukhodolov, A. N., & Rowinski, P. M. (1997). Statistical sand wave dynamics in one-directional water flows. *Journal of Fluid Mechanics*, *351*, 17–39.

Nordin, C., & Algert, J. (1966). Spectral analysis of sand waves. *Journal of the Hydraulics Division*, *92*, 95–114.

Olinde, L., & Johnson, J. P. L. (2015). Using RFID and accelerometer-embedded tracers to measure probabilities of bed load transport, step lengths, and rest times in a mountain stream. *Water Resources Research*, *51*, 7572–7589.

Pähtz, T., & Durán, O. (2018). The cessation threshold of nonsuspended sediment transport across aeolian and fluvial environments. *Journal of Geophysical Research. Earth Surface*, *123*, 1638–1666.

Paola, C., & Voller, V. (2005). A generalized Exner equation for sediment mass balance. *Journal of Geophysical Research*, *110*, F04014.

Papanicolaou, A. N., Elhakeem, M., Krallis, G., Prakash, S., & Edinger, J. (2008). Sediment transport modeling review—current and future developments. *Journal of Hydraulic Engineering*, *134*, 1–14.

Parker, G., Paola, C., & Leclair, S. (2000). Probabilistic Exner sediment continuity equation for mixtures with no active layer. *Journal of Hydraulic Engineering*, *126*, 818–826.

Pelosi, A., Schumer, R., Parker, G., & Ferguson, R. I. (2016). The cause of advective slowdown of tracer pebbles in rivers: Implementation of Exner-Based Master Equation for coevolving streamwise and vertical dispersion. *Journal of Geophysical Research. Earth Surface*, *121*, 623–637.

Recking, A. (2013). An analysis of nonlinearity effects on bed load transport prediction. *Journal of Geophysical Research*, *118*, 20090.

Revil-Baudard, T., & Chauchat, J. (2013). A two-phase model for sheet flow regime based on dense granular flow rheology. *Journal of Geophysical Research: Oceans*, *118*, 619–634. doi:10.1029/2012JC008306

Richardson, E. V., Simons, D. B., & Posakony, G. J. (1961). *Sonic depth sounder for laboratory and field use* (Vol. Circular 450). Washington, DC: United States Geological Survey.

Rickenmann, D. (1990). *Bedload transport capacity of slurry flows at steep slopes* (Technical Report No. 103). Mitteilungen 103 der Versuchanstalt für Wasserbau, Hydrologie und Glaziologie.

Savage, S. (1984). The mechanics of rapid granular flows. *Advances in Applied Mechanics*, *24*, 289–366.

Schumer, R., Meerschaert, M. M., & Bauemer, B. (2009). Fractional advection-dispersion equations for modeling transport at the Earth surface. *Journal of Geophysical Research. Earth Surface*, *114*. doi:10.1029/2008JF001246

Seminara, G., & Bolla Pittaluga, M. (2012). Reductionist versus holistic approaches to the study of river meandering: An ideal dialogue. *Geomorphology*, *163-164*, 110–117.

Seminara, G., Solari, L., & Parker, G. (2002). Bed load at low Shields stress on arbitrary sloping beds: failure of the Bagnold hypothesis. *Water Resources Research*, *38*, 1249.

Simons, D. B., Richardson, E. V., & Nordin, C. F. (1965). *Bedload equation for ripples and dunes* (Technical Report No. Professional Paper 462 H). U.S. Geological Survey.

Simons, D. B., & Şentük, F. (1992). *Sediment transport technology: Water and sediment dynamics* (2nd ed. Littleton, CO: Water Resources Publication.

Singh, A., Lanzoni, S., Wilcock, P. R., & Foufoula-Georgiou, E. (2011). Multiscale statistical characterization of migrating bed forms in gravel and sand bed rivers. *Water Resources Research*, *47*, W12526.

Smart, G., & Jaeggi, M. (1983). *Sedimenttransport in steilen Gerinnen* (Technical Report No. 64). Mitteilungen 64 der Versuchanstalt für Wasserbau, Hydrologie und Glaziologie.

Smith, B., Clifford, N. J., & Mant, J. (2014). The changing nature of river restoration. *Wiley Interdisciplinary Reviews: Water*, *1*, 249–261.

van der Mark, C., Blom, A., & Hulscher, S. (2008). Quantification of variability in bedform geometry. *Journal of Geophysical Research*, *113*, F03020.

Vischer, D. (2003). *Die Geschichte des Hochwasserschutzes in der Schweiz* (Technical Report No. Berichte des BWG. Serie Wasser BWGW Nr. 5). Bundesamt für Umwelt BAFU.

Voller, V. R., & Paola, C. (2010). Can anomalous diffusion describe depositional fluvial profiles? *Journal of Geophysical Research: Earth Surface*, *115*, F00A13.

Wainwright, J., Parsons, A. J., Cooper, J. R., Gao, P., Gillies, J. A., Mao, L., . . . P. G. Knight (2015). The concept of transport capacity in geomorphology. *Reviews of Geophysics*, *53*, 1155–1202.

Wiberg, P. L., & Smith, J. D. (1989). Model for calculating bedload transport of sediment. *Journal of Hydraulic Engineering*, *115*, 101–123.

Wilcock, P. (1997). Entrainment, displacement and transport of tracer gravels. *Earth Surface Processes and Landforms*, *22*, 1125–1138.

Wohl, E., Angermeier, P., Bledsoe, B., Kondolf, G., MacDonnel, L., Merritt, D., . . . Tarboton, D. (2005). River restoration. *Water Resources Research*, *41*, W10301.

Wong, M., & Parker, G. (2006). Reanalysis and correction of bed-load relation of Meyer-Peter and Müller using their own database. *Journal of Hydraulic Engineering*, *132*, 1159–1168.

Wong, M., Parker, G., DeVries, P., Brown, T., & Burges, S. (2007). Experiments on dispersion of tracer stones under lower-regime plane-bed equilibrium bed load transport. *Water Resources Research*, *43*, W03440.

Wu, Z., Foufoula-Georgiou, E., Parker, G., Singh, A., Fu, X., & Wang, G. (2019). Analytical solution for anomalous diffusion of bedload tracers gradually undergoing burial. *Journal of Geophysical Research. Earth Surface*, *124*, 21–37.

Yalin, M. (1972). *Mechanics of sediment transport*. Oxford: Pergamon Press.

Zhang, Y., Meerschaert, M. M., & Packman, A. I. (2012). Linking fluvial bed sediment transport across scales. *Geophysical Research Letters*, *39*, L20404.